Available online at www.sciencedirect.com
ScienceDirect
Journal of Nuclear Materials 373 (2008) 119–122
journal of nuclear materials
www.elsevier.com/locate/jnucmat

Laser Raman microprobe analysis of graphite exposed to edge plasma in the TEXTOR tokamak

T. Hirai [a,*], J. Compan [a], K. Niwase [b], J. Linke [a]

[a] IEF 2, Forschungszentrum Jülich GmbH, EURATOM Association, 52425 Jülich, Germany
[b] Hyogo University of Teacher Educations, Hyogo 673-1494, Japan

Received 12 October 2006; accepted 16 May 2007

Abstract

An isotropic fine grain graphite (EK98) block has been exposed to the edge plasma in the TEXTOR tokamak and studied by Raman spectroscopy. Spectra from the net erosion area and deposition area where co-deposits (hard layer) were created by the tokamak discharges, are remarkably different. The spectra at the net erosion areas consist of two sharp peaks: the D-peak ($\approx$1355 cm^{-1}) and the G-peak ($\approx$1580 cm^{-1}). The spectra at the net deposition areas were very broad, which are similar to the Raman spectra of amorphous carbon. Fitting analyses of the Raman spectra for the net erosion area exhibit a linear relationship between the G-peak width ($FWHM_G$) and the peak intensity ratio (I_D/I_G). Comparison with the diagram derived for ion-irradiated graphite revealed that thermally unstable defects of single vacancies scarcely remained due to the power loading in this plasma exposure condition but thermally stable defects such as the dislocation dipoles could be accumulated.

1. Introduction

Carbon-based materials (CBMs) are favourable for fusion applications because of a low atomic number, good thermo-mechanical properties, low coefficient of thermal expansion and the absence of melting. Fine grain graphites are used in numerous existing fusion devices, and advanced CBMs, carbon fibre composites (CFCs), are the candidate material for the vertical targets of the ITER divertor, where heat and particle fluxes are the highest [1]. The load with energetic particles such as neutrons causes radiation damage in CBMs which leads to a reduction of the thermal conductivity [2], whereas the high heat flux loads will raise the temperature of CBMs and may cause an annealing of the radiation damage.

Raman spectroscopy is sensitive to the graphitic structures (phonon distribution) [3] and has been applied in order to study the structural changes of CBMs. Various CBMs, e.g. fine grain graphite, pyrolytic graphite, diamond, CFC, glassy carbon, were characterized after neutron irradiation [4,5], ion irradiation [5–9] and electron beam loading [10,11] together with undamaged original grades [9,12–14].

To evaluate the effect of intense plasma loading on the damage accumulation, in the present paper, a fine grain graphite block was exposed to the edge plasma in the TEXTOR tokamak and studied by Raman spectroscopy.

2. Experimental

An isotropic fine grain graphite (EK98) block was machined as a test limiter with dimensions of 120 mm in the toroidal direction and 80 mm in the poloidal direction and with a spherical surface 70 mm radius. The block was mounted on the limiter lock system and exposed to the edge plasma in the TEXTOR tokamak in Forschungszentrum Jülich. The typical plasma parameters are a line-averaged electron density $n_e = 2-6 \times 10^{13}$ m^{-3}, plasma current $I_p = 330$ kA and a power of the neutral beam

* Corresponding author. Tel.: +49 2461 61 5843; fax: +49 2461 61 3699.
E-mail address: t.hirai@fz-juelich.de (T. Hirai).

0022-3115/$ - see front matter © 2007 Elsevier B.V. All rights reserved.
doi:10.1016/j.jnucmat.2007.05.040

injection $P_{NBI} = 1.8$ MW. The details of the plasma exposure experiments were described elsewhere [15]. The graphite block was exposed to 29 discharges (5–6 s plasma exposure for each discharge, shot number #91142–#91170) at the last closed flux surface (LCFS, $r = 46$ cm) and 5 mm outside of LCFS ($r = 46.5$ cm) in the tokamak. The typical edge plasma parameters were, $n_e \approx 2 \times 10^{18}$ m^{-3}, $T_e \approx 100$ eV. The highest ion flux and heat load at the spherical limiter surface were estimated to be 7×10^{22} ions/(m^2 s) and 9 MW/m^2, respectively. This corresponds to an integrated ion fluence to approximately 1×10^{25} ions/m^2. The limiter temperature was measured by thermocouples. The bulk temperature increased from 300 °C to 400 °C during the experimental campaign and the maximum surface temperature has been estimated to be slightly above 1500 °C at the end of discharges.

After the plasma exposure, the test limiter was investigated by micro-Raman spectroscopy, using a backscattering geometry with the 488.0 nm line of the Ar-ion laser. The beam spot had a diameter of 2 μm. Although the nominal grain size of the EK98 grade is 7–12 μm, the microstructure of the test limiter has not been taken into account for the measurements as the Raman spectra did not show any significant micro-scale dependence. The analysis depth (d) was calculated by the absorption coefficient (α) of the laser light in matters. The absorption coefficient of a 488 nm (2.55 eV) photon in low hydrogen-containing deposits (high density > 1.64 g/cm^3) has been evaluated to be 6×10^6 m^{-1} [16]. Hence, the analysis depth is calculated to be 83 nm ($d = 1/(2\alpha)$). The analysis depth should be larger in deposits with the higher hydrogen contents. The analysis depth in the isotropic fine grain graphite, on the other hand, is considered to be in a range of 40–50 nm, judging from the optical skin depth of a laser with similar wavelength, 514.5 nm (2.42 eV) [17,18].

3. Results

Fig. 1. shows an optical micrograph of the test limiter after the plasma exposure in the TEXTOR tokamak. The areas at the highest heat load look darker than the neighboring areas. The micro-Raman measurements were performed along the toroidal direction, indicated by a scale attached on the limiter surface. Typical Raman spectra from three different areas of the plasma-exposed limiter surface are shown in Fig. 2. They correspond to (a) the highly loaded area, namely, net erosion area, at 52 mm from the limiter edge at the ion drift side, (b) the net deposition area at 20 mm from the limiter edge and (c) the rear surface of the limiter, which corresponds to the Raman spectrum of the original graphite grade. The Raman spectra from the highly loaded area and the rear surface area exhibit two clear peaks, which correspond to the graphite peak (G-peak, E_{2g} Raman active mode) around 1580 cm^{-1} and the disordered peak (D-peak, originated by non-zero-centre phonon) around 1355 cm^{-1} [3]. The spectra could be deconvoluted into two sharp Lorenzian peaks with a least-squares

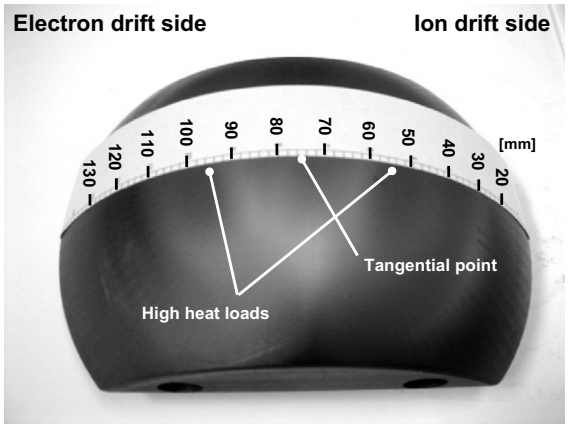

Fig. 1. Image of the test limiter exposed to the edge plasma in the TEXTOR tokamak. A scale is attached for positioning of micro-Raman measurements.

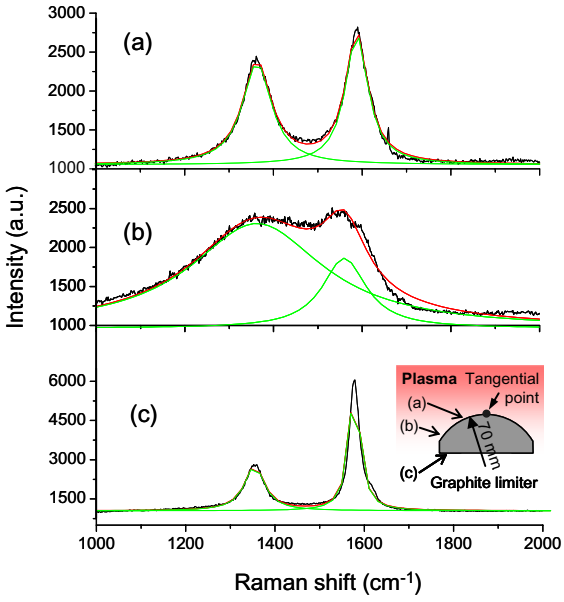

Fig. 2. Typical Raman spectra from the graphite limiter surfaces of (a) the highly loaded part in the net erosion area, (b) the net deposition area, (c) the rear side of the graphite limiter, indicating the Raman spectrum from the original grade.

algorithm as shown in Fig. 2. The Raman spectrum from the net deposition area created by the tokamak discharges, on the other hand, exhibits a very broad intensity distribution, which can be fitted by two Gaussian peaks at the above mentioned wave numbers.

Fig. 3. displays the variation of the Raman intensity ratio (I_D/I_G), which was deduced by deconvolution along the toroidal direction. The horizontal axis shows the position on the limiter surface from the ion drift side to the electron drift side. The value of I_D/I_G obtained from the rear surface of the limiter is indicated by a horizontal bar ($I_D/I_G = 0.24$–0.4) as the original grade of graphite. The central area between 3.5 and 11.5 cm corresponds to a net erosion area which was exposed to plasma more

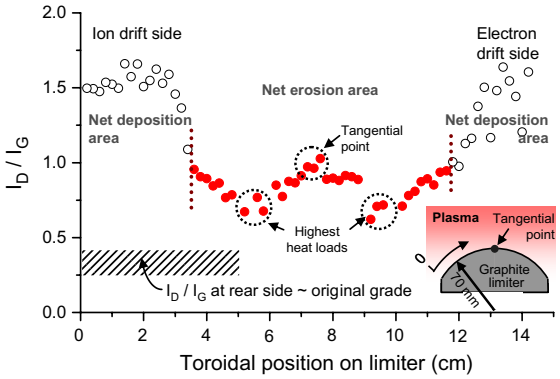

Fig. 3. Variation of Raman intensity ratios (I_D/I_G) of the graphite limiter along the toroidal direction after plasma exposure.

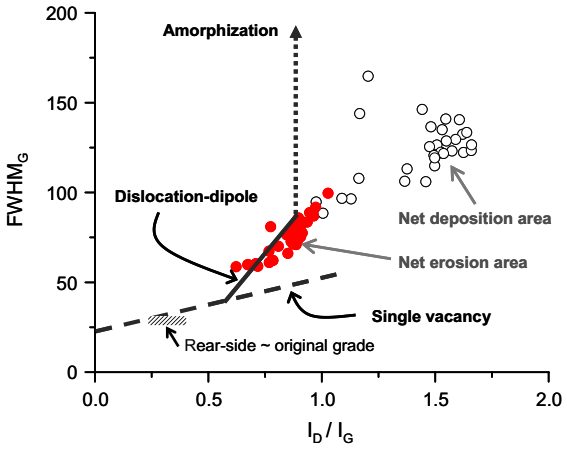

Fig. 4. Change of G-peak width ($FWHM_G$) as a function of the intensity ratio (I_D/I_G) after irradiation of HOPG with He ions [5,7]. The diagram has been analyzed in terms of the formation of single vacancies and disordered regions (dislocation dipoles) [18]. The data obtained from the graphite test limiter are plotted as closed (net erosion area) and open circles (net deposition area) in the diagram.

intensively as this area is closer to the plasma center. The lateral edges located at the positions at 0–3.5 cm, and 11.5–14 cm, on the other hand, correspond to the net deposition areas. There is a typical heat flux profile at the limiter surface due to (1) the radial decay of the heat flux outside LCFS in the tokamak, (2) the projection of the heat flux onto the spherical limiter surface. The largest temperature increases were observed in position at 5.5 cm and 9.5 cm. A rather moderate temperature increases were found in the centre of the limiter (7.5 cm at the tangential point) and at the lateral sides of the limiter (the net deposition area).

4. Discussion

Here the Raman spectra of the plasma-exposed limiter are interpreted in terms of defect formation and plasma impurity effects, etc. One should note that the intensity ratio of I_D/I_G in the net erosion area is higher than the value of the original grade as shown in Fig. 3. This means that the plasma exposure in the TEXTOR tokamak leads to the introduction of defects in the surface of graphite limiter. It has been widely accepted that the value of I_D/I_G for various grades of graphite behave inversely proportional against the 'crystallite size L_a' [14]. However, in irradiated graphite, the change of I_D/I_G cannot be explained simply by the change of L_a but by the accumulation of in-plane defects of single vacancies and some in-plane defects which can induce disordering of the basal plane [7,19]. It should be noted that the thermal stability of the two types of defects is different: single vacancy can mutually annihilate with interstitials by annealing below 873 K but not for another defect [20]. By assigning another defect to dislocation dipole, the dimensional change and the Raman intensity ratio under irradiation could be well explained by a kinetic model [21]. The dislocation dipoles nucleate via the relaxation and stabilization of di-vacancies and grow linearly by knock-on process [22].

To clarify the nature of defects formed in the graphite limiter, we utilize the diagram of the relation between the full width at half maximum of the G-peak, $FWHM_G$ and the peak intensity ratio, I_D/I_G as shown in Fig. 4. This diagram was derived by a systematic investigation on the change of Raman spectra for highly oriented pyrolytic graphite (HOPG) specimens irradiated with He ions at temperatures between RT and 973 K [5,7]. The dash-line corresponds to the accumulation of single vacancies due to Frenkel-pair production. The solid line, on the other hand, shows the change of Raman spectra for HOPG specimens irradiated above 573 K. Below 473 K, the upward deviation from the dashed line starts at higher values of I_D/I_G compared to the values above 573 K. This is due to the smaller annealing effect of Frenkel pairs, which allows single vacancies to accumulate to high concentration. Then, an increase of the I_D/I_G along the solid line means a gradual increase of the concentration of thermally stable defects of dislocation dipoles. The dotted line corresponds to the amorphization of the graphite structure [5,7] due to a remarkable accumulation of dislocation dipoles [21,22].

The present data obtained from the graphite limiter are plotted in the diagram. Notably, the data from the net erosion area follow the solid-line. This is consistent with the case of ion irradiation as the bulk temperature of the limiter graphite was estimated to be in a range from 573 K to 673 K under the loading condition. It means that defects generated during plasma exposures are mostly thermally stable defects, i.e. dislocation dipoles. Changes of I_D/I_G in the net erosion area can also be explained by the local variation of the temperature under plasma loading. The I_D/I_G value exhibits minima at the highest power loading points and maximum around the tangential point as shown in Fig. 3. This indicates that an increase of surface temperature induced by higher loads enhances the annealing of point defects, thus, leading to a reduced formation of defect clusters such as dislocation dipoles.

The Raman spectra from the co-deposits created by the tokamak discharges, on the other hand, show remarkable

broad peaks as shown in Fig. 2(b). According to the previous experiments in TEXTOR, the deposits grow typically at a rate of 2–3 nm/s [23]. Thus, deposits created by 174 s (29 shots of 6 s discharge) tokamak-discharge will have a thickness of around 350–520 nm. Therefore, it is evident that the Raman analysis was done mainly within the deposits, judging from the analysis depths for graphite and hydrogen-containing deposits. This is consistent with the spectra obtained at the net deposit area, which show no additional sharp peaks expected from the substrate graphite under deposit layer.

The co-deposits of hydrogen isotopes (hydrogen (H) and deuterium (D)) and carbon (C), have various characteristic properties depending on the plasma parameters and the substrate temperature. Commonly, the hydrogenated carbon deposits are classified in two groups: (i) the hard layer with high density ($\approx$2.0 g/cm^3), which has a low H(D)/C ratio ($\approx$0.4), and (ii) the soft (polymer-like) layer with low density ($\approx$1.1 g/cm^3), which has a high H(D)/C ratio ($\approx$1) [24]. The H(D)/C ratio of the co-deposits created at the limiter surface in similar experimental conditions are around 0.4 or less [25]. Therefore, the studied co-deposits are supposed to be hard layers and the broad Raman peaks should reflect a disordered carbon structure in the layer. Dedicated studies of such co-deposits could be carried out with Fourier Transform Infrared (FTIR) spectroscopy by observing directly the C–H vibrational bands [24].

Also, it should be mentioned that Rutherford backscattering spectrometry (RBS) has revealed the existence of metallic impurities such as boron, copper, tungsten at the limiter surface [15]. These impurities originated from the boronization processes which were used for wall-conditioning [26] and from a simultaneous experimental program with a test limiter made out of a castellated W/Cu [15]. However, significant feature attributed to metallic elements and their compounds have not appeared in the Raman spectra.

5. Conclusions

A test limiter made from fine grain graphite was exposed to the edge plasma in the TEXTOR tokamak and observed by Raman spectroscopy. The net erosion and net deposition areas are clearly classified by the characteristic peaks in Raman spectra. The Raman spectra in the net erosion area consist of two sharp Lorenzian peaks, those in the deposition area consist of broad Gaussian peaks. The detailed analysis of the Raman spectra from the net erosion area indicates that the defects induced during plasma exposures are mostly thermally stable defects, i.e. dislocation dipoles. This is probably due to the increase of the surface temperature during plasma exposure, enhancing the annihilation of thermally unstable point defects of single vacancies with interstitials. The broad Raman peak from the net deposition area reflects a disordered graphitic structure, which originates from hard layers of co-deposition from hydrogen isotopes and carbon.

Acknowledgements

Authors would like to thank Drs G. Sergienko and A. Kreter for discussions on the plasma exposure experiments in the TEXTOR tokamak.

References

[1] T. Hirai, K. Ezato, P. Majerus, Mater. Trans. 46 (2005) 412.
[2] M. Roedig, W. Kuehnlein, J. Linke, D. Pitzer, M. Merola, E. Rigal, B. Schedler, E. Visca, J. Nucl. Mater. 329–333 (2004) 766.
[3] R. Al-Jishi, G. Dresselhaus, Phys. Rev. B 26 (1982) 4514.
[4] K. Niwase, K. Nakamura, T. Shikama, T. Tanabe, 170 (1990) 106.
[5] T. Tanabe, T. Maruyama, M. Iseki, K. Niwase, H. Atsumi, Fus. Eng. Des. 29 (1995) 428.
[6] E.S. Elman, M. Shayegan, M.S. Dresselhaus, H. Mazurek, G. Dresselhaus, Phys. Rev. B 25 (1982) 4142.
[7] K. Niwase, T. Tanabe, Mater. Trans. 34 (1993) 1111.
[8] K. Niwase, Y. Kakimoto, I. Tanaka, T. Tanabe, Nucl. Instrum. and Meth. B 91 (1994) 78.
[9] N. Kangai, T. Tanabe, K. Niwase, J. Nucl. Mater. 212–215 (1994) 1234.
[10] M. Kitajima, M. Fujitsuka, H. Shinno, J. Mater. Sci. Lett. 9 (1990) 19.
[11] T. Tanabe, K. Niwase, Y. Miyamoto, I. Tanaka, M. Seki, M. Akiba, M. Arai, H. Shinno, M. Fujitsuka, Y. Kubota, J. Nucl. Mater. 176&177 (1990) 467.
[12] K. Ashida, K. Kanamori, K. Watanabe, J. Vac. Sci. Technol. A6 (1988) 2232.
[13] T. Tanabe, K. Niwase, N. Tsukuda, E. Kuramoto, J. Nucl. Mater. 191–194 (1992) 330.
[14] F. Tunstra, J.L. Koenig, J. Chem. Phys. 53 (1970) 1126.
[15] T. Hirai, V. Philipps, A. Huber, G. Sergienko, J. Linke, T. Wakui, T. Tanabe, M. Rubel, M. Wada, T. Ohgo, et al., J. Nucl. Mater. 313–316 (2003) 69.
[16] F.W. Smith, J. Appl. Phys. 55 (1984) 764.
[17] D.-Q. Yang, E. Sacher, Surf. Sci. 504 (2002) 125.
[18] J. Liu, M.D. Hou, C. Trautmann, R. Neumann, C. Müller, Z.G. Wang, Q.X. Zhang, Y.M. Sun, Y.F. Jin, H.W. Liu, H.J. Gao, Nucl. Instrum. and Meth. B 212 (2003) 303.
[19] K. Niwase, Phys. Rev. B 52 (1995) 15785.
[20] K. Niwase, I. Tanaka, T. Tanabe, J. Nucl. Mater. 191–194 (1992) 335.
[21] K. Niwase, Philos. Mag. Lett. 82 (2002) 401.
[22] K. Niwase, Mater. Sci. Eng. A 400–401 (2005) 101.
[23] P. Wienhold, M. Rubel, M. Mayer, D. Hildebrandt, W. Schneider, A. Kirschner, Phys. Scripta T94 (2001) 141.
[24] W. Jacob, Thin Solid Films 326 (1998) 1.
[25] V. Philipps, A. Pospieszczyk, A. Huber, A. Kirschner, J. Rapp, B. Schweer, P. Wienhold, G. van Oost, G. Sergienko, T. Tanabe, K. Ohya, M. Wada, T. Ohgo, M. Rubel, J. Nucl. Mater. 258–263 (1998) 858.
[26] J. Winter, H.G. Esser, L. Könen, V. Philipps, H. Reimer, J.v. Seggern, J. Schlüter, E. Vietzke, F. Waelbroeck, P. Wienhold, T. Banno, D. Ringer, S. Veprek, J. Nucl. Mater. 162–164 (1989) 713.